Magnetic interaction of Co ions near the $(10\bar{1}0)$ ZnO surface

2010 New J. Phys. 12 083061

(http://iopscience.iop.org/1367-2630/12/8/083061)

New Journal of Physics
The open-access journal for physics

Magnetic interaction of Co ions near the $(10\bar{1}0)$ ZnO surface

Thomas Archer[1], **Chaitanya Das Pemmaraju and Stefano Sanvito**
School of Physics and CRANN, Trinity College, Dublin 2, Ireland
E-mail: archert@tcd.ie

New Journal of Physics **12** (2010) 083061 (14pp)
Received 12 March 2010
Published 31 August 2010
Online at http://www.njp.org/
doi:10.1088/1367-2630/12/8/083061

Abstract. Co-doped ZnO is the prototypical dilute magnetic oxide, showing many of the characteristics of ferromagnetism. The microscopic origin of the long-range order, however, remains elusive, since the conventional mechanisms for magnetic interaction, such as super-exchange and double exchange, fail either at the fundamental or at a quantitative level. Intriguingly, there is growing evidence that defects both in point-like and in extended form play a fundamental role in driving the magnetic order. Here, we explore one such possibility by performing *ab initio* density functional theory calculations for the magnetic interaction of Co ions at or near a ZnO $(10\bar{1}0)$ surface. We find that extended surface states can hybridize with the *e*-levels of Co and efficiently mediate the magnetic order, although such a mechanism is effective only for ions placed in the first few atomic planes near the surface. We also find that the magnetic anisotropy changes at the surface from a hard-axis easy plane to an easy axis, with an associated increase in its magnitude. We then conclude that clusters with high densities of surfacial Co ions may display blocking temperatures much higher than in the bulk.

[1] Author to whom any correspondence should be addressed.

Contents

1. Introduction

Dilute magnetic semiconductors (DMSs) [1] are a new class of materials in which transition metal (TM) dopants (usually Co, Fe or Mn) replace native cations in ordinary semiconductors. The TMs provide localized spins, and in some cases free carriers, and the material often displays evidence of ferromagnetism at remarkably low TM concentrations and relatively high temperatures. The expectation about DMSs is that they might offer the advantages of semiconductors (e.g. an easy-to-manipulate electronic structure), together with the non-volatility of ferromagnets. In short, they may be an ideal materials platform for future 'spintronics' technologies [2].

(Ga,Mn)As is by far the most studied of the DMSs, mostly because of its compatibility with present GaAs/AlAs technology. However, despite more than a decade of refinements in the synthetic method and of improvement of the annealing treatments to control the various defect concentrations, the (Ga,Mn)As Curie temperature is still far from exceeding room temperature [3], hindering the prospect for mainstream applications. These difficulties have moved the focus of experimental activity towards other host materials and in particular towards oxides-based DMSs [4] such as ZnO.

The most commonly used dopant in this case is Co and at present the claims for room temperature ferromagnetism in ZnO:Co, following the first exciting report from Ueda *et al* [5], are numerous (for an up-to-date review published in 2008, see [6] and references therein). The experimental literature, however, is populated with controversial results and almost all possible magnetic phases have been found in samples with the same nominal Co concentration that have been grown under apparently similar conditions. Thus, together with ferromagnetism [7], paramagnetism [8, 9] and a spin-glass behavior [10] have also been reported in the past.

Some of the early claims of ferromagnetism were, however, affected by an incomplete materials characterization. This has now been considerably improved, and more recent studies that concentrate on a careful search for secondary phases generally fall under two categories: either a ferromagnetic signal is observed resulting from metallic cobalt [11]–[14], or the material is paramagnetic [8, 9, 15, 16]. However, there are still studies being published where the analysis has shown no magnetic clusters, and yet the magnetic signal appears to persist [17]–[20]. However, it is important to point out that in most of these experiments the samples undergo gas treatment of some kind before the magnetism is detected.

Such a phenomenology, together with the fact that often ultra-high-quality ZnO:Co films lack ferromagnetism even for large n-doping conditions [9, 15, 16], indicates that the ferromagnetic signal, when observed in the absence of secondary phases[2], must be related to the presence of crystallographic defects, either in their point-like or macroscopic form. Such a hypothesis was brought forward to explain the reversible detection of a magnetic signal, not correlated to the sample conductivity, upon subsequent oxidation and reduction of ZnO:Co samples [21] (note that secondary phase analysis was not carried out in this work). A similar line of thought was used to critically re-analyze a multitude of published data for ZnO:Mn and to correlate the appearance of magnetism to a large surface-to-volume ratio of the sample grains [22].

With the conventional mechanisms for the magnetic interaction, such as super- and double exchange, failing either at the qualitative or quantitative level [23], most of the theoretical activity in the field has concentrated on first principles methods, in particular on density functional theory (DFT). Early calculations for ZnO doped with extremely high concentrations of Co (25%) predicted a room temperature ferromagnetic ground state in the absence of additional dopants [24, 25]. These concentrations, however, are above the percolation threshold for nearest-neighbor magnetic interaction, so that even a short-range mechanism such as super-exchange can, in principle, yield ferromagnetism. Below such a threshold, where essentially all the experiments are conducted, one should expect at best only super-paramagnetic clusters [6].

Furthermore, it is important to point out that for this rather complicated problem, one should take particular care when choosing the exchange and correlation functional to use in DFT. The standard local density and generalized gradient approximations (LDA and GGA, respectively) severely underestimate the native ZnO gap and misplace in energy the Co d levels. Both effects contribute to predicting spurious long-range ferromagnetism. Rigorous corrections based on energy considerations [26, 28, 29] improve the description and return a picture of antiferromagnetic interaction among nearest-neighbor Co ions and little interaction at any other distance [6]. Thus, also, theory points to defects as a source of magnetism or at least as a tool to boost either the strength or the range of the magnetic interaction.

For instance, uncompensated spins on the surface of secondary CoO phases have been proposed as the origin for the experimentally observed magnetic hysteresis [30]. This essentially means attributing the observed ferromagnetism to super-paramagnetically blocked clusters. However, this proposal was also rejected at the quantitative level by DFT calculations. In fact, the calculated order temperatures of cubic, wurtzite and zinc-blende CoO polymorphs are all well below room temperature [31], with finite size effects not playing any particular role [32].

Another possibility is represented by complexes involving Co ions and native ZnO intrinsic defects. This was examined in great detail by Pemmaraju *et al* [6], who concluded that only complexes of O vacancies (V_O) and substitutional Co ions can couple magnetically to a medium range if additional n-type doping is present. Other defect combinations can provide remarkably large local magnetic interaction, but provide no long-range interaction. A phase diagram was then proposed where the various magnetic states could be mapped out onto the relative abundance of Co ions and Co–V_O complexes. Although it is often claimed that the presence of V_O in magnetic samples is suggestive, it is not clear whether the concentrations

[2] Note that even when no secondary phases have been observed, one cannot categorically exclude the presence of defects either not measurable by the characterization techniques used or in concentrations too small to be detected.

of Co–V_O complexes needed for room temperature ferromagnetism are achievable in reality [33].

The theoretical study of ZnO surfaces may hold the key to understanding the experimental results. The polar (0001) and (000$\bar{1}$) surface of ZnO:Co has previously been studied using the LSDA functional [47]; however, using the LSDA functional for such a study is questionable. The LSDA functional places the t_2 level too low in the conduction band, leading to an unrealistic ferromagnetic ground state even for the bulk ZnO:Co system in the dilute limit [6].

In this work, we investigate whether magnetism can arise at a ZnO open surface. We have chosen the most stable surface to study, namely the non-polar (10$\bar{1}$0) surface. If this is proved true, then the theory will also converge in establishing a link between the macroscopic morphology of samples and their magnetism.

2. Calculation details

All our calculations are performed using DFT. The standard local and semi-local exchange and correlation functionals (LDA and GGA) are not appropriate for the description of the electronic structure of ZnO and CoO [6]. We have therefore opted for an approximated form of the self-interaction correction scheme (ASIC) [34], which has been shown to correctly reproduce the electronic structure of ZnO:Co [6], in good agreement with spectroscopical data. The ASIC method is included in a development version of the local atomic orbital basis set DFT code *Siesta* [35]. For all our calculations, we use the value of $\alpha = \frac{1}{2}$ for the ASIC potential scaling parameter. α behaves as an effective screening parameter within the ASIC correction; $\alpha = 1$ produces good results for small molecules and atoms, whereas $\alpha = 0$, i.e. no ASIC correction, is appropriate for the limit of the free electron gas. $\alpha = \frac{1}{2}$ provides a good description of the electronic structure of strongly correlated insulators and semiconductors, away from the purely ionic limit [34].

The electron density and the Hamiltonian for the valence electrons are described by a double-ζ polarized (DZP) basis set. Core electrons are replaced by standard norm-conserving Troullier–Martins pseudopotentials. The real space integration grid has an spacing equivalent to an 800 Ryd plane-wave cut-off, while the reciprocal space sampling is performed over a grid with an equivalent real space distance of 15 Å. The forces are calculated from the LDA Ceperley–Alder [36] functional using the ASIC density [37], and all structures are relaxed to less than 0.01 eV Å^{-1}.

3. Undoped ZnO surface

The wurtzite structure of bulk ZnO is well described by the ASIC method: both the in-plane, **a**, and the out-of-plane, **c**, lattice parameters are slightly contracted with respect to experiments. In particular, they are calculated to be, respectively, 3.209 and 5.180 Å, as against the reported values of 3.252 and 5.313 Å. The distortion parameter u is found to be 0.380 after relaxation, which is essentially identical to its experimental value of 0.382 [38].

The (10$\bar{1}$0) is the most stable and frequently occurring ZnO [39] surface; it is not polar, since it contains both Zn and O atoms. The unit cell for the surface is constructed from the primitive cell of bulk ZnO and is illustrated in figure 1. Due to the non-polar nature of the surface, we found it unnecessary to passivate the side of the slab opposite to the one that gets

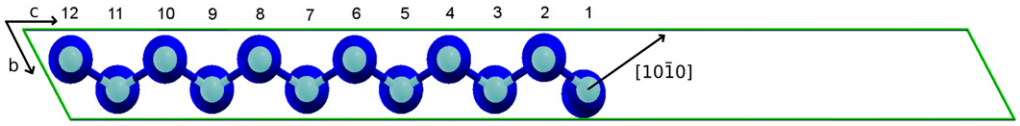

Figure 1. Relaxed unit cell used to describe the ZnO (10$\bar{1}$0) surface: the point of view is along the **a** axis. The numbers label the different atomic layers as used throughout in the present paper. The large dark blue balls represent Zn, whereas the small light green ones are for O.

doped with Co; instead we have chosen to keep the bottom four layers of the slab fixed to the bulk crystal structure during relaxation. Furthermore, when performing further relaxation, we always constrain the cell geometry and allow only the atomic positions to relax. A vacuum region of 10 Å is sufficient to prevent the interaction between slab periodic images, and in fact a further increase of the length of the vacuum region produces a less than 1 meV change in the total energy. A slab thickness of 17.7 Å (12 atomic layers totaling 24 atoms) is found to be sufficient to encompass surface relaxations with a less than 5 meV Å^{-1} change in the maximum force upon introduction of further layers.

In order to test for surface reconstructions a 2×2 surface cell is created. The atoms, excluding those fixed to their ZnO bulk positions, are randomly displaced by a displacement of up to 0.5 Å. The cell is then allowed to relax; it is found to revert back to the unit cell structure (with no reconstruction). Therefore, in the absence of any obvious surface reconstruction, we continue to assume that the primitive surface unit cell can be simply constructed from the primitive ZnO bulk unit cell.

The relaxation due to the surface causes a compression of the slab by 3.3%. The uppermost Zn atom relaxes into the slab more than the oxygen by $\Delta d_\perp = 0.167$ Å, causing a tilting of the Zn–O pair of 5°. In the second layer, the amplitude of the tilting is reduced and the direction of tilting is reversed, giving $\Delta d_\perp = -0.075$ Å. Subsequent layers have $\Delta d_\perp$ values of 0.043, -0.018 and 0.008 Å, respectively. Experimentally, the relaxation of the (10$\bar{1}$0) surface remains controversial [40] with $d_\perp$ ranging from 0.4 ± 0.1 Å [41] to -0.12 ± 0.06 Å [42].

In general, the formation of the (10$\bar{1}$0) surface reduces the coordination of both O and Zn from 4 to 3 in the top layer, while, of course, the remaining atoms retain their bulk coordination number. This results in a modification of both the electronic structure and the atomic positions in the vicinity of the surface. In figure 2, we present the difference, $\Delta\rho$, between the Mülliken charges calculated for the surfaces with respect to that of bulk ZnO as a function of the layer position (distance from the surface). We can clearly observe that there is a charge re-arrangement in the topmost three atomic layers. This is more pronounced at the surface (layer 1), where O increases its Mülliken valence charge by $0.03e$ (e is the electron charge), mainly due to the enhanced population of the 2p orbitals. Of course, such an enhancement does not correspond to doping (the O p shell is already completely filled), but simply to a re-arrangement of the atomic and the overlap Mülliken populations, i.e. to a reduction of the Zn–O hybridization at the surface. In contrast, the Zn Mülliken charge is reduced by $0.06e$, the majority of which comes from the 4p orbital. Interestingly, the nominal Mülliken population for bulk ZnO is already reached after four monolayers for both Zn and O, indicating that the perturbation of the electronic structure interests only the surface.

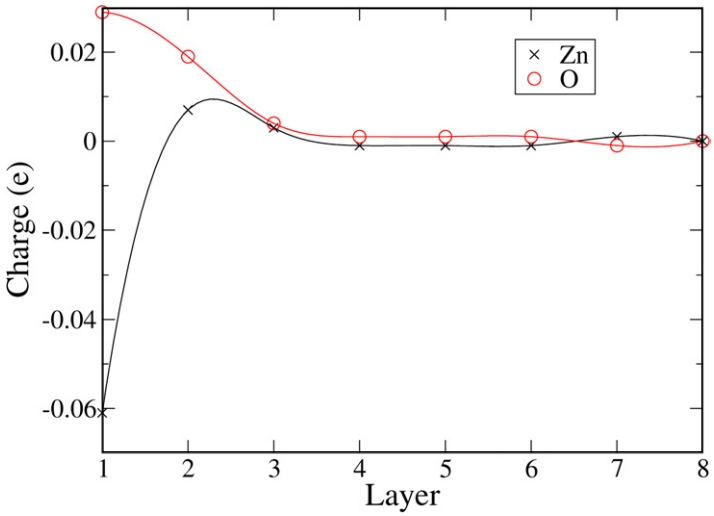

Figure 2. Change in the Mülliken charge, $\Delta\rho$, with respect to the ZnO bulk value in the first atomic layers of the $(10\bar{1}0)$ surface. The index labeling the position of the atomic layers follows the definition of figure 1.

Further information can be obtained by comparing the density of states (DOS) of the surface super cell with that of bulk ZnO (see the top panel of figure 3(a)). Together with an increase of the Zn d DOS bandwidth, the main feature of the surface DOS is the presence of a split-off band just at the top of the valence band. This is almost entirely due to O p states and it is localized near the surface. In figure 3(b), we present the isosurface corresponding to the local DOS of such a surface state. This corresponds to the charge density distribution of energy levels placed within a narrow energy window around the valence band top (yellow dashed region in figure 3(a)). Clearly, the figure confirms the presence of an O-derived surface state. Finally, we note that additional surface states appear at the ZnO conduction band bottom and, as a consequence, the ZnO band gap is reduced from 3 to 2.5 eV.

4. Co defects in ZnO

Cobalt ions enter the ZnO lattice as substitutional defects sitting at the Zn site. Their electronic structure, and in particular the position of the empty t_2 states, is still a matter of debate [26], although there is agreement that beyond LDA, DFT methods are necessary to capture the insulating nature of ZnO:Co. As mentioned previously, here we use ASIC DFT, which returns an electronic structure in good agreement with UPS data [27]. As an example, the DOS of a 128-atom bulk ZnO cell including a single Co ion is presented in figure 3(a) (middle panel). One can clearly see that the filled minority e states lie near the ZnO valence band top, while the first resonant t_2 level is well within the conduction band [6]. With such an electronic structure, n-type doping will not open a double exchange channel, while p-type doping is notoriously difficult in ZnO. Therefore, as it stands, bulk ZnO:Co in the absence of other defects cannot sustain a long-range magnetic interaction.

We now twin our attention to investigating the effect of the surface on the Co electronic structure and its magnetic interaction. In this case, a single Co ion is introduced into the slab at

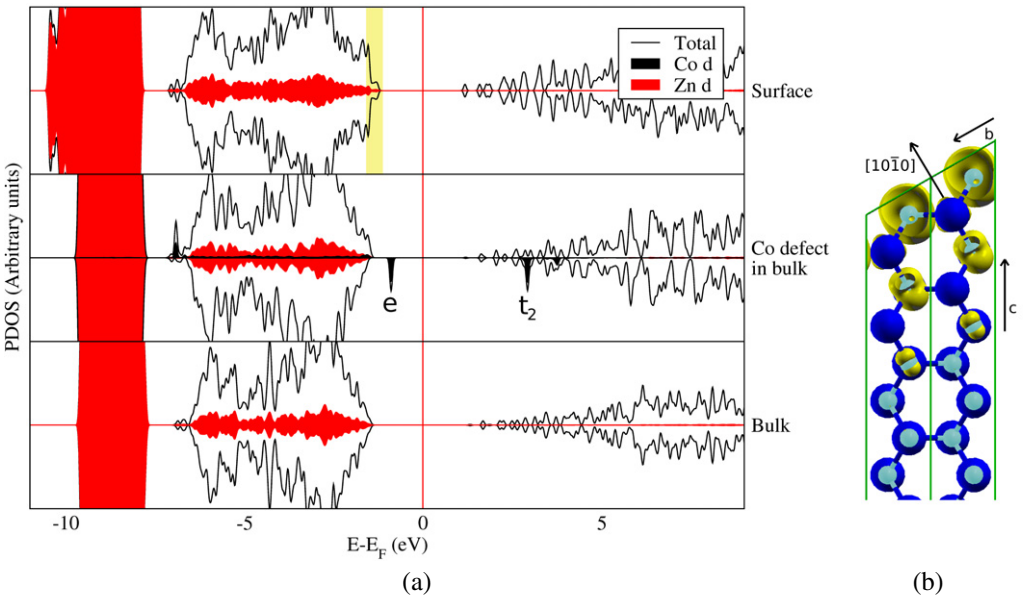

Figure 3. Electronic structure of the ZnO (10$\bar{1}$0) surface. In panel (a) we show the DOS for the (10$\bar{1}$0) surface (top panel), bulk ZnO (bottom panel) and bulk ZnO-doped Co at the Zn site (middle panel). The positive DOSs are for the majority electrons, while the negative are for the minority. The energy region marked in yellow in the top panel indicates the energy window used to calculate the local DOS of (b). Note the rather localized surface state with amplitude mainly on the O ions. The color code for the atoms in panel (b) is the same as that of figure 1.

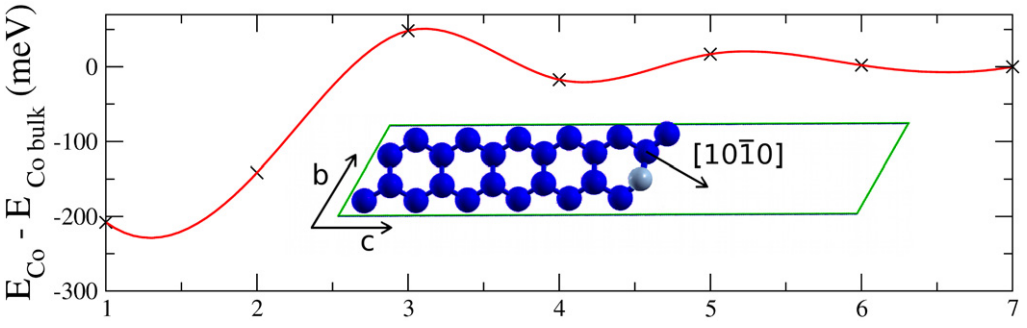

Figure 4. Energy for incorporating a substitutional Co defect into the ZnO lattice near the (10$\bar{1}$0), calculated for a single Co atom in a 2×2 slab. The surface slab for a substitutional Co atom in layer 1 is shown in the inset. The energy is plotted with zero being the energy for including the Co ion in layer 7.

different substitutional positions. We use for these calculations a 2×2 slab (comprising 96 atoms), which corresponds to a total $Zn_{1-x}Co_xO$ doping of $x = 0.021$. Note, however, that the Co concentration in plane is rather high, since in a single ZnO atomic layer, one out of four Zn is replaced by Co. The cell is always relaxed with the exception of the four bottom layers, which are kept at their bulk coordinates. In figure 4, we plot the energy that a Co ion gains by

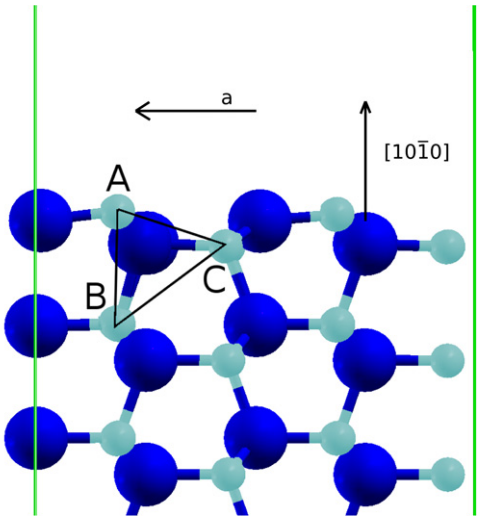

Figure 5. A view along **b** showing the distorted oxygen tetrahedron for a Co atom in layer 2.

moving from the bulk to the surface. This is calculated as the total energy difference between a given supercell and that where Co occupies layer 7 in the slab. A dipole is observed for these slab calculations; however, this dipole remains relatively constant for all the calculations; an error of only 5 meV is observed for the worst case, when the Co atom is placed in the top layer. Clearly, there is a substantial reduction of the total energy as Co moves closer to the (10$\bar{1}$0) surface, indicating that Co segregation to the surface is likely if the ions possess enough kinetic energy during the growth.

The electronic structure of Co near the (10$\bar{1}$0) surface is investigated next in figure 6, where we present the DOS of the slab as a function of the Co position. We can observe a substantial interaction between the surface states and the Co d levels, both at the valence band top and within the conduction band. This is rather strong for the two inequivalent positions at the (10$\bar{1}$0) surface (layers 1 and 2), where a substantial broadening of both the e and t_2 peaks is observed. In particular, when Co is placed on layer 2, which corresponds to the cation site close to the surface with the full tetrahedral coordination, shown in figure 5. There is a substantial majority d DOS appearing in the ZnO gap and, in general, all the d manifold is pushed rather high in energy, so that the native ZnO band gap is almost entirely filled. This can be understood from the distortion of the coordinating oxygen tetrahedron. The Co atom relaxes to a position closer to the surface, reducing the bond length to the two surface O to 1.89 Å (denoted as 'A' in figure 5) and increasing the bond length to the deepest O to 2.00 Å ('B'). The bond length of the remaining O ('C') remains unchanged from the bulk value of 1.96 Å. This difference in bond length lifts the degeneracy of the d orbitals and results in a smeared DOS. As the Co moves away from the surface, the DOS resembles more closely a superposition between the DOS of the surface and that of Co doped in the bulk of ZnO. Interestingly, for all the positions investigated, the orbital degeneracy of minority e states remains lifted by the interaction with the surface state at the valence band top. Again, with the only exception of Co doping in the first two surface layers, such an electronic structure is not favorable for sustaining long-range magnetic interaction.

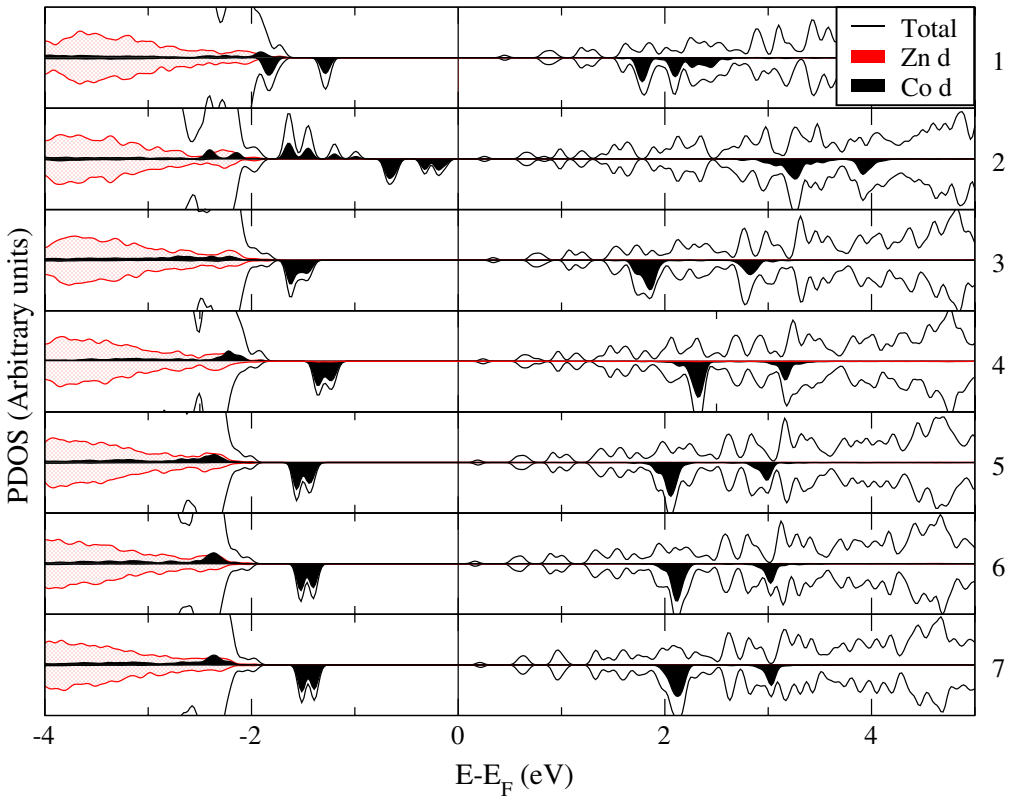

Figure 6. DOS and orbital-projected DOS (PDOS) for a slab including a single Co ion as a function of the distance from the exposed $(10\bar{1}0)$ surface. The number on the right-hand side is the layer index, so that 1 corresponds to Co doped in the first layer, 2 corresponds to Co doped in the second layer and so on. Note that the surface state produces significant changes in the Co DOS only when Co is placed in the first two topmost layers, i.e. at the $(10\bar{1}0)$ surface.

5. Surface-mediated magnetic coupling

We next move on to study the magnetic coupling between Co ions placed in the two topmost layers close to the $(10\bar{1}0)$ surface. In general, we find that the magnetic interaction is strongly dependent on the precise mutual position of the defects and of the free surface. As such, it is necessary to span a large number of possible Co positions. In order to perform this analysis, we construct from the relaxed supercell discussed in section 4 a 4×3 surface cell including two substitutional Co ions doped in the two topmost layers. In order to make the calculations numerically more feasible, our constructed cell contains only six atomic layers, a number sufficient to keep the forces at the surface within 0.01 eV Å^{-1}. This is equivalent to an overall Co concentration of about 4%, which is a value easily achievable in experiments (again it should be noted that the concentration of Co is highly inhomogeneous, i.e. it is very large at the surface).

The exchange coupling is then calculated with the broken symmetry approach, i.e. by comparing the DFT total energy for the same cell, when the magnetic moments of the two Co ions are aligned either ferromagnetically, E_{FM}, or antiferromagnetically, E_{AF}, with respect to each other. The energy difference $E_{\mathrm{AF}} - E_{\mathrm{FM}}$ is then a measure of the magnetic interaction.

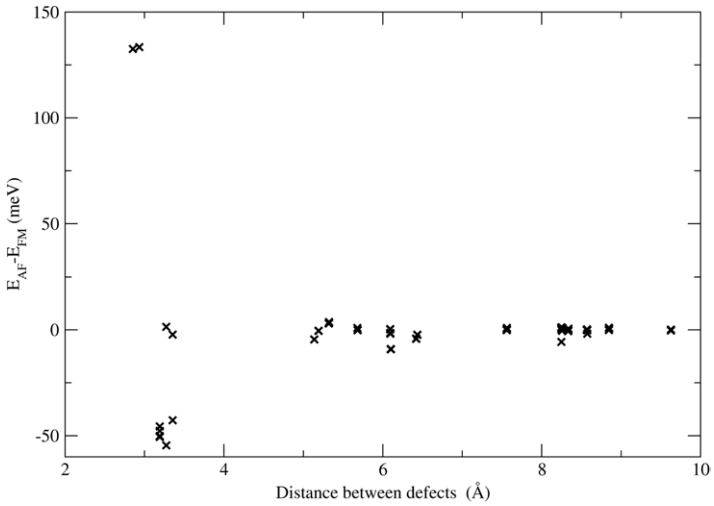

Figure 7. Difference between the total energies of the ferromagnetic (E_{FM}) and antiferromagnetic (E_{AF}) configuration of a cell containing two Co ions as a function of the distance between the ions $d_{Co–Co}$.

The results of this analysis are summarized in figure 7, where $E_{AF} - E_{FM}$ is plotted against the distance between the two Co centers, $d_{Co–Co}$. The main features are the presence of two distinct regions of strong magnetic coupling, respectively ferromagnetic and antiferromagnetic, for short $d_{Co–Co}$, and the almost complete absence of long-range magnetic interaction. Thus, unless further doped, the $(10\bar{1}0)$ surface does not seem to offer a more favorable picture in terms of exchange coupling than the bulk, with strong close-distance interaction and essentially no long-range features. Thus, also in this case, long-range ferromagnetism must be excluded. However, whether or not superparamagnetic blocked clusters can form in abundance and mimic a ferromagnetic hysteresis signal remains an open question, whose answer sensitively depends on the likely Co concentration achievable on the surface and the Co magnetic anisotropy. This will be discussed next and put into perspective in section 7.

Going into more details of the magnetic interaction, we find that strong ferromagnetic coupling ($E_{AF} - E_{FM} > 0$) is associated with nearest-neighbor Co ions, the first being placed right at the surface and the second in the second layer, and exchanged coupled through an O also at the surface. In contrast, the configurations having strong antiferromagnetic interaction ($E_{AF} - E_{FM} < 0$) are characterized by having the mediating O atom sitting on the second layer from the surface and the two Co ions placed either both on the surface or one on the surface and one in the second layer. This suggests that in principle a specific pattern of magnetic order should be possible if one is able to control the absorption site of the Co ions on the surface.

6. Anisotropy

In general, the breaking of the crystal field symmetry at a surface is expected to increase the magnetic anisotropy, as for instance in the case of Co on Pt for which the massive zero-field splitting of 9.3 meV has been reported [43]. For Co doped in bulk ZnO the value for the zero-field splitting, D, is 2.76 cm^{-1} (0.34 meV) [8, 44], with Co having an hard axis along the wurtzite crystallographic **c** axis and an easy plane (the **a**–**b** plane). This is consistent with

model Hamiltonian calculations for TMs in trigonally distorted tetrahedral coordination [45]. With such a high anisotropy and assuming a certain degree of frustration, we have previously estimated that superparamagnetic particles comprising more than 250 Co ions should be blocked at room temperature [6]. The question is now whether magneto-crystal anisotropy at the surface can reduce the size of cluster needed to produce a blocked superparamagnetic cluster.

In order to calculate the magneto-crystal anisotropy, we use a 2×2 surface cell containing four atomic layers for a total of 32 atoms and where one surface Zn ion is replaced by Co. An equivalent cell, although with periodic boundary conditions along the three dimensions, is used for the bulk calculations. The anisotropy is computed from *Siesta* DFT by using an on-site approximation for the spin–orbit matrix elements [46]. This requires a non-collinear calculation, which unfortunately cannot be performed with the ASIC method, since at present it is only defined for collinear DFT. Therefore, all the anisotropy calculations are carried out at the LDA level by using the Ceperley–Alder [36] functional. In practice, we compute the total energy as a function of the direction of the Co magnetic moment with respect to the wurtzite **c** axis.

The results of our calculations are presented in figure 8(a), where we report the total energy, E, as a function of the angle, ϕ, between the magnetization and the wurtzite **c** axis. In the figure, we present three cases, namely that of Co in bulk ZnO, of wurtzite CoO [32] and the Co-doped $(10\bar{1}0)$ surface. For both the bulk ZnO:Co and wurtzite CoO, we predict a hard axis along the crystallographic wurtzite **c** direction and an easy plane perpendicular to this axis, in agreement with experiments.

For the bulk, the zero-field splitting parameter is estimated by a simple fit of our data to the DS_z^2 Hamiltonian, where S_z is the component of the spin along the hard (z) axis. If we take S as a classical vector (as in DFT), such a Hamiltonian can be rewritten in the form $D|S^2|\cos^2(\phi)$. By fitting the curve in figure 8(a) to a $\cos^2$ curve and by assuming $|S| = 3/2$, we find $D = 0.71$ meV. This result is essentially identical for both the wurtzite CoO and the substitutional Co in the ZnO lattice; however, it is approximately a factor of two larger than what is found in experiments. We are at present uncertain of the reason for such a discrepancy. This may lie in the choice of the LDA functional, which usually overestimates the p–d hybridization, or in the on-site approximation to the spin–orbit matrix elements or in the crude way in which we extract the parameter.

Even with this uncertainty, it is still useful to compare the bulk anisotropy to that of Co on the surface. We find that the surface changes the nature of the anisotropy drastically. The Co ions placed at the under-coordinated position on the surface now have an easy axis oriented at 120° from the wurtzite **c** axis, as shown in figure 8(b). The zero field splitting is calculated as 2.18 meV, i.e. it is approximately a factor of three larger than that in the bulk. This gives us a quite remarkably high anisotropy, which pushes the limit for superparamagnetic clusters blocked at room temperature down to about 80 atoms. This means that we need approximately 80 Co atoms, magnetically coupled (i.e. in nearest-neighbor positions) on the surface, in order to have a cluster displaying magnetic hysteresis at room temperature.

7. Concluding remarks

We have studied the electronic structure, magnetic interaction and magnetic anisotropy of Co ions at or in the vicinity of the $(10\bar{1}0)$ ZnO surface, in the search for an explanation of the often claimed room temperature ferromagnetism in ZnO:Co. Our results give a contrasting picture.

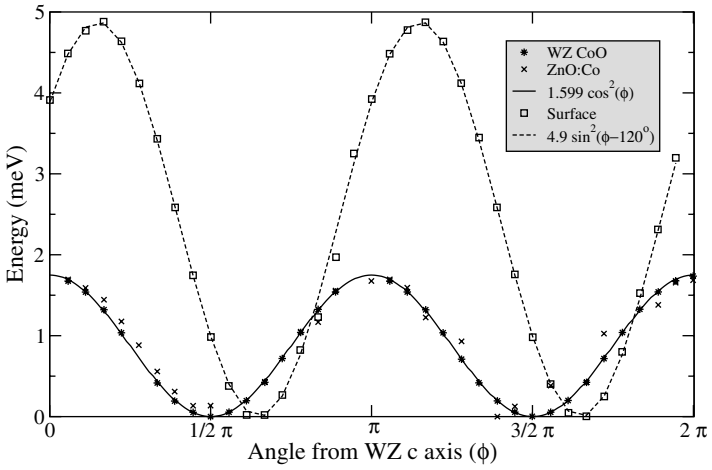

(a)

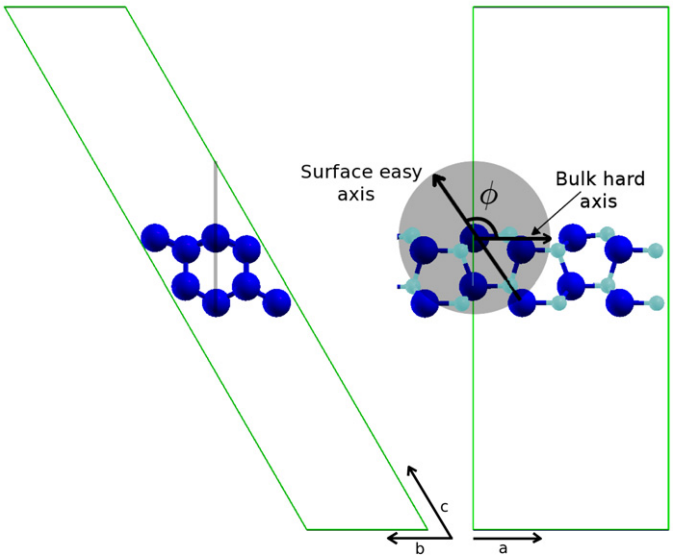

(b)

Figure 8. (a) Total energy, E, as a function of the angle ϕ between the Co magnetic moment and the wurtzite **c** axis. The calculations are performed for Co in a bulk ZnO matrix (ZnO:Co), for wurtzite CoO (WZ CoO) and for a Co ion at the $(10\bar{1}0)$ ZnO surface (surface). (b) The path taken by the magnetic moment for the surface cell. Note that $\phi = 0$ corresponds to the bulk **c** direction.

On the one hand, we have found that the magnetic interaction is rather strong for atoms that sit on the surface, which is in some circumstances ferromagnetic in nature. Moreover, there is a substantial energy gain for a single Co ion to locate at the surface, so that high superficial Co densities might be expected in nanoparticles and granular materials, i.e. in objects with a large surface-to-volume ratio. On the other hand, we have also found that the magnetic interaction remains extremely short-ranged, which means that the surface does not act as an extended defect mediating the magnetic coupling. This aspect is not different from what happens in bulk

ZnO and excludes the presence of long-range room temperature ferromagnetism. Certainly, the situation might change in the case of polar surfaces, or when surface doping is possible.

There are, however, a few more facts to consider. Firstly, the magnetic anisotropy at the $(10\bar{1}0)$ surface is enhanced threefold with respect to its bulk value and it changes from the hard-axis easy plane to the easy axis. This means that superparamagnetic clusters formed at the surface will block at a much higher temperature than in bulk. Alternatively, one can say that for the same blocking temperature, much smaller clusters are required at the surface to mimic a ferromagnetic signal. This is indeed an attractive perspective that may validate the uncompensated spin model proposed by Dietl *et al* [30]. Using a rather crude estimate of the size of superparamagnetically blocked clusters at room temperature, we predict that approximately 80 atoms are required. This means that one needs up to 80 atoms connected by a nearest-neighbor percolation path on the $(10\bar{1}0)$ surface. Considering that the two-dimensional percolation threshold ranges from 1/2 to about 0.7 depending on the particular surface, we can conclude that the majority of the surface Zn sites should be replaced by Co in order to have magnetic hysteresis at room temperature.

The probability of such a cluster occurring on the surface of a dilute phase is low. However, we have shown that it is energetically favorable for the ions to migrate to the surface; this, coupled with a less than perfect growth method, may cause the regions of high Co concentration necessary for the ferromagnetic signal to be observed.

Acknowledgments

This work was sponsored by the Science Foundation Ireland and the EU FP7 project ATHENA. We thank HPC-Europa and TCHPC for computational support.

References

[1] Dietl T, Ohno H, Matsukura F, Cibert J and Ferrand D 2000 *Science* **287** 1019
[2] Wolf S A *et al* 2001 *Science* **294** 1488
[3] Novák V *et al* 2008 *Phys. Rev. Lett.* **101** 077201
[4] Coey J M D 2006 *Curr. Opin. Solid State Mater. Sci.* **10** 83
[5] Ueda K, Tabata H and Kawai T 2001 *Appl. Phys. Lett.* **79** 988
[6] Pemmaraju C D, Hanafin R, Archer T, Braun H B and Sanvito S 2008 *Phys. Rev.* B **78** 054428
[7] Tuan A C *et al* 2004 *Phys. Rev.* B **70** 054424
[8] Sati P *et al* 2006 *Phys. Rev. Lett.* **96** 017203
[9] Ney A, Ollefs K, Ye S, Kammermeier T, Ney V, Kaspar T C, Chambers S A, Wilhelm F and Rogalev A 2008 *Phys. Rev. Lett.* **100** 157201
[10] Peng Y Z, Liew T, Chong T C, Song W D, Li H L and Liu W 2005 *J. Appl. Phys.* **98** 114909
[11] Jedrecy N, von Bardeleben H J and Demaillie D 2009 *Phys. Rev.* B **80** 205204
[12] Opel M, Nielsen K W, Bauer S, Goennenwein S T B, Cezar J C, Scheeisser D, Simon J, Mader W and Gross R 2008 *Eur. Phys. J.* B **63** 437–44
[13] Heald S M *et al* 2009 *Phys. Rev.* B **79** 075202
[14] Ney A *et al* 2010 *New J. Phys.* **12** 013020
[15] Kaspar T C, Droubay T, Heald S M, Nachimuthu P, Wang C M, Shutthanandan V, Johnson C A, Gamelin D R and Chambers S A 2008 *New J. Phys.* **10** 055010
[16] Chambers S A 2010 *Adv. Mater.* **22** 219
[17] Xu Q *et al* 2008 *Appl. Phys. Lett.* **92** 082508

[18] Singhal R K, Samariya A, Kumar S, Xing Y T, Deshpande U P, Shripathi T and Baggio-Saitovitch E 2010 *J. Magn. Magn. Mater.* **322** 2187
[19] Liu Y and MacManus-Driscoll J L 2009 *Appl. Phys. Lett.* **94** 022503
[20] Kim S J, Lee S, Cho Y C, Choi Y N, Park S, Jeong I K, Kuroiwa Y, Moriyoshi C and Jeong S-Y 2010 *Phys. Rev.* B **81** 212408
[21] Khare N, Kappers M J, Wei M, Blamire M G and MacManus-Driscoll J L 2006 *Adv. Mater.* **18** 1449
[22] Straumal B B, Mazilkin A A, Protasova S G, Myatiev A A, Straumal P B, Schütz G, van Aken P A, Goering E and Baretzky B 2009 *Phys. Rev.* B **79** 205206
[23] Hanafin R and Sanvito S 2007 *J. Magn. Magn. Mater.* **316** 218
[24] Sato K and Katayama-Yoshida H 2000 *Japan. J. Appl. Phys. II Lett.* **39 6B** L555
[25] Sato K and Katayama-Yoshida H 2002 *Phys. Status Solidi* b **229** 673
[26] Sanvito S and Pemmaraju C D 2009 *Phys. Rev. Lett.* **102** 159701
[27] Kobayashi M *et al* 2005 *Phys. Rev.* B **72** 201201
[28] Lany S, Raebiger H and Zunger A 2008 *Phys. Rev.* B **77** 241201
[29] Gopal P and Spaldin N A 2006 *Phys. Rev.* B **74** 094418
[30] Dietl T, Andrearczyk T, Lipińska A, Miecana M, Tay M and Wu Y 2007 *Phys. Rev.* B **76** 155312
[31] Archer T, Hanafin R and Sanvito S 2008 *Phys. Rev.* B **78** 014431
[32] Hanafin R, Archer T and Sanvito S 2010 *Phys. Rev.* B **81** 054441
[33] Kobayashi M *et al* 2010 arXiv:1001.0712
[34] Pemmaraju C D, Archer T, Sánchez-Portal D and Sanvito S 2007 *Phys. Rev.* B **75** 045101
[35] Soler J M, Artacho E, Gale J D, García A, Junquera J, Ordejón P and Sánchez-Portal D 2002 *J. Phys.: Condens. Matter* **14** 2745
[36] Ceperley D M and Alder B J 1980 *Phys. Rev. Lett.* **45** 566
[37] Droghetti A and Sanvito S 2009 *Appl. Phys. Lett.* **94** 252505
[38] Decremps F, Datchi F, Saitta A M and Polian A 2003 *Phys. Rev.* B **68** 104101
[39] Wander A, Schedin F, Steadman P, Norris A, McGrath R, Turner T S, Thornton G and Harrison N M 2001 *Phys. Rev. Lett.* **86** 3811
[40] Meyer B and Marx D 2003 *Phys. Rev.* B **67** 035403
[41] Duke C B, Meyer R J, Paton A and Mark P 1978 *Phys. Rev.* B **18** 4225
[42] Jedrecy N, Gallini S, Sauvage-Simkin M and Pinchaux R 2000 *Surf. Sci.* **460** 136
[43] Gambardella P *et al* 2003 *Science* **300** 1130
[44] Estle T L and de Wit M 1961 *Bull. Am. Phys. Soc.* **6** 445
[45] Kuzian R O, Daré A M, Sati P and Hayn R 2006 *Phys. Rev.* B **74** 155201
[46] Fernándes-Seivane L, Oliveira M A, Sanvito S and Ferrer J 2006 *J. Phys.: Condens. Matter* **18** 7999
[47] Sanchez N, Gallego S and Muñzo M C 2008 *Phys. Rev. Lett.* **101** 067206